Polymer Journal, Vol. 24, No. 10, pp 1155—1164 (1992)

NMR Measurements of Identical Polymer Samples by Round Robin Method III. Analysis of Frequency Dependences of ^{13}C Spin-Lattice Relaxation Times and Nuclear Overhauser Enhancements

Fumitaka HORII, Masaru NAKAGAWA, Ryozo KITAMARU,
Riichirô CHÛJÔ,* Koichi HATADA,**
and Yasuyuki TANAKA***,†

Institute for Chemical Research, Kyoto University,
Uji, Kyoto 611, Japan
** Department of Material Engineering, The Nishi-Tokyo University,*
Uenohara-cho, Kita-Tsuru-gun,
Yamanashi 409-01, Japan
*** Department of Chemistry, Faculty of Engineering Science,*
Osaka University, Toyonaka, Osaka 560, Japan
**** Department of Material Systems Engineering, Faculty of Technology,*
Tokyo University of Agriculture and Technology,
Koganei, Tokyo 184, Japan

(Received May 15, 1992)

ABSTRACT: The frequency dependences of ^{13}C spin-lattice relaxation times (T_1) and nuclear Overhauser enhancements (NOE) of poly(methyl methacrylate) (PMMA) in $CDCl_3$ solution have been analyzed in terms of different models describing the motions of the C–H internuclear vector. Box-type and log-χ^2 distribution models of correlation times as well as the 2τ model assuming two independent motions are inadequate to explain simultaneously the frequency dependences of T_1 and NOE values for backbone CH_2, α-CH_3, and OCH_3 carbons. In contrast, those frequency dependences can be well interpreted by the 3τ model in which three superimposed motions with correlation times of the orders of 10^{-12}, 10^{-10}, and 10^{-9} s are assumed. This indicates that the backbone motion of PMMA should be described in terms of at least three types of superimposed motion and thus one or two additional motions may be overlapped for the side-group carbons.

KEY WORDS ^{13}C NMR / Poly(methyl methacrylate) / Round Robin Method / Spin-Lattice Relaxation Time / Nuclear Overhauser Enhancement / Frequency Dependence / Molecular Motion /

The local motions of polymers in solution have been investigated by a number of spectroscopic techniques. Among these techniques ^{13}C NMR spectroscopy is very powerful in analyzing the detailed motions for the respective carbon nuclei which constitute polymeric

† The following names should be succeeded as the coauthors: S. Amiya (*Kuraray Central Research Laboratory*), T. Asakura (*Tokyo University of Agriculture and Technology*), K. Chikaishi (*Sumitomo Chemical Co. Ltd.*), Y. Goto (*University of Tokyo*), K. Hikichi (*Hokkaido University*), Y. Hirakida (*Showa Denko K.K.*), S. Hosoda (*Sumitomo Chemical Co., Ltd.*), M. Imanari (*JEOL Ltd.*), S. Itoh (*Kyoto University*), M. Kamachi (*Osaka University*), T. Kawamura (*University of Tokyo*), T. Kitayama (*Osaka University*), S. Kohjiya (*Kyoto Institute of Technology*), K. Lee (*Osaka University*), I. Nagoya (*Asahi Chemical Industry Co.*), Y. Oka (*Mitsui Toatsu Chemicals, Inc.*), T. Okada (*Tosoh Corporation*), M. Okumura (*Toa Nenryo Kogyo Kabushikigaisha*), T. Saito (*Nippon Oil Company, Ltd.*), H. Sato (*Tokyo University of Agriculture and Technology*), T. Sei (*Daicel Chemical Industries, Ltd.*), T. Seimiya (*Idemitsu Kosan Co.*), T. Shiibashi (*Japan Synthetic Rubber Co.*), T. Shimamura (*Nitto Technical Information Center Co., Ltd.*), M. Shimoda (*Nippon Zeon Co., Ltd.*), Y. Takai (*Osaka University*), H. Tanaka (*Okayama University*), Y. Terawaki (*Osaka University*), T. Usami (*Mitsubishi Petrochemical Co.*), K. Ute (*Osaka University*), T. Yonemitsu (*Kyushu Sangyo University*).

chains.[1-3] It is, however, difficult to measure the frequency dependences of NMR relaxation parameters over a wide range of frequency, because each NMR spectrometer is operated normally at a fixed frequency under a fixed magnetic field. Under such a situation no appropriate model for motions of polymers has been developed yet particularly for data obtained in solution, although many models have been proposed in the respective cases.

In order to overcome this difficulty, a cooperative project was proposed for members as well as non-members of Research Group on NMR of the Society of Polymer Science, Japan (SPSJ). In the second paper of this series,[4] we examined the reliability of ^{1}H and ^{13}C spin-lattice relaxation times (T_1) and nuclear Overhauser enhancements (NOE) by round robin method using a poly(methyl methacrylate) (PMMA) solution as an identical sample. Although different members measured them at different frequencies corresponding to ^{1}H Larmor frequencies from 60 to 500 MHz on 27 spectrometers, the precision was 5—10% for ^{1}H and ^{13}C T_1s as well as for NOE values at each frequency. In this paper, therefore, we analyze the frequency dependences of ^{13}C T_1s and NOE thus obtained in terms of different models describing the thermal fluctuation of the C–H internuclear vector and discuss about the characteristic local motion of PMMA in solution. The preparation and characterization of the PMMA sample are described in the first paper of this series.[5] The triad tacticity and molecular weight of the polymer are as follows; $mm=0.04$, $mr=0.347$, $rr=0.613$, and $\bar{M}_n$ (GPC) $=27400$, $\bar{M}_n$ (VPO) $=28500$, $\bar{M}_w$ (GPC) $=58000$. A review of this series, including a preliminary analysis of the frequency dependences, has been published elsewhere.[6]

ANALYSIS

In the natural abundant ^{13}C–^{1}H two spin system, where the ^{13}C spin relaxation is dominated by the ^{13}C–^{1}H dipolar interaction, ^{13}C T_1 and NOE may be expressed as

$$\frac{1}{NT_1}=\frac{\gamma_H^2\gamma_C^2\hbar^2}{16r^6}\{J_0(\omega_H-\omega_C)+18J_1(\omega_C)+9J_2(\omega_H+\omega_C)\} \tag{1}$$

$$\mathrm{NOE}=1+\frac{9J_2(\omega_H+\omega_C)-J_0(\omega_H-\omega_C)}{J_0(\omega_H-\omega_C)+18J_1(\omega_C)+9J_2(\omega_H+\omega_C)}\cdot\frac{\gamma_H}{\gamma_C} \tag{2}$$

where N is the number of protons chemically bonded to ^{13}C nuclei and γ_H and γ_C are the nuclear gyromagnetic ratios of ^{1}H and ^{13}C nuclei, respectively. $\hbar$ is the reduced Planck constant ($=h/2\pi$), r is the distance between ^{1}H and ^{13}C nuclei, and ω_H and ω_C are the ^{1}H and ^{13}C Larmor frequencies, respectively. In these equations $J_q(\omega)$ are the spectral density functions, which are defined as the Fourier transforms of the autocorrelation functions of the orientation functions $F_q(t)$ at frequency ω:

$$J_q(\omega)=\int_{-\infty}^{\infty}\langle F_q^*(t+\tau)F_q(t)\rangle\exp(-i\omega\tau)\mathrm{d}\tau \tag{3}$$

with $q=0$, 1, and 2. The orientation functions $F_q(t)$ are given by

$$\begin{aligned}F_0(t)&=1-3n^2\\F_1(t)&=(l+im)n\\F_2(t)&=(l+im)^2\end{aligned} \tag{4}$$

Here, l, m, and n are the direction cosines of the C–H internuclear vector with respect to the x, y, and z axes in the laboratory frame, respectively, the z axis being parallel to the direction of the static magnetic field. Although $J_q(\omega)$'s are calculated for many different models describing molecular motions of polymers, the

following models are examined in this paper.

Single-Correlation-Time Model

The C–H internuclear vector undergoes a spherically random motion and then $J_q(\omega)$ are expressed as

$$J_q(\omega)=K_q\frac{2\tau_c}{1+\omega^2\tau_c^2} \tag{5}$$

with

$$\begin{aligned} K_0&=4/5\\ K_1&=2/15\\ K_2&=8/15 \end{aligned} \tag{6}$$

Distribution of the Correlation Times

In order to describe the complicated motions of polymers the distribution of the correlation times is frequently considered. In that case the spectral densities are given by

$$J_q(\omega)=K_q\int_0^\infty \frac{2P(\tau_c)\tau_c}{1+\omega^2\tau_c^2}\,d\tau_c \tag{7}$$

with $\int_0^\infty P(\tau)d\tau=1$. In this paper the following two types of distributions are elucidated.

Box-type distribution:[7]

$$\ln P(\ln\tau_c)=\begin{cases}\ln(\ln\tau_c)^{-1} & \tau_{cs}\leqq\tau_c\leqq\varepsilon\tau_{cs}\\ -\infty & \text{otherwise}\end{cases} \tag{8}$$

Then

$$J_q(\omega)=\frac{2k_q}{\omega\ln(\varepsilon)}\times\tan^{-1}\frac{\omega\bar{\tau}\ln(\varepsilon)}{1+\varepsilon(\varepsilon-1)^{-2}(\ln(\varepsilon))^2\omega^2\bar{\tau}^2} \tag{9}$$

where $\bar{\tau}$ is the average correlation time.

log-χ^2 distribution:[8]

$$P(s)\,ds=\frac{1}{\Gamma(p)}(ps)^{p-1}e^{-ps}\,ds \tag{10}$$

where p is a parameter to determine the width of distribution and s is given by

$$s=\log_b[1+(b-1)\tau_c/\bar{\tau}] \tag{11}$$

Here b is the adjustable parameter of 10—1000. In this case $J_q(\omega)$ are numerically calculated using the following equation.

$$J_q(\omega)=K_q\int_0^\infty\frac{2\bar{\tau}P(s)(b^s-1)\,ds}{(b-1)\left\{1+\omega^2\bar{\tau}^2\left[\frac{(b^s-1)}{(b-1)}\right]^2\right\}} \tag{12}$$

Multiple-Correlation-Time Models

In multiple-correlation-time models the thermal fluctuation of the C–H internuclear vector is described in terms of the superposition of several independent random motions.[9,10] Let $O_1, O_2, \cdots, O_{p-1}$ be the rectangular coordinates which are placed in the respective moving units. Here denote by O_1 the coordinate system to describe the most local motion of the C–H internuclear vector and by O_p the laboratory frame. The direction cosines l, m, and n in the laboratory frame are then related to the direction cosines l_1, m_1, and n_1 of the C–H vector in coordinate O_1 by the following equation:

$$\begin{pmatrix} l\\ m\\ n\end{pmatrix}=T_p\cdots T_3T_2\begin{pmatrix} l_1\\ m_1\\ n_1\end{pmatrix} \tag{13}$$

where T_j are the matrices of the orthogonal transformation from coordinate O_{j-1} to coordinate O_j:

$$T_j=\begin{pmatrix} \cos\phi_j\cos\theta_j\cos\psi_j-\sin\phi_j\sin\psi_j & -\cos\phi_j\cos\theta_j\sin\psi_j-\sin\phi_j\sin\theta_j & \cos\phi_j\sin\theta_j\\ \sin\phi_j\cos\theta_j\cos\psi_j+\cos\phi_j\sin\psi_j & -\sin\phi_j\cos\theta_j\sin\psi_j+\cos\phi_j\cos\psi_j & \sin\phi_j\sin\theta_j\\ -\sin\theta_j\cos\psi_j & \sin\theta_j\sin\psi_j & \cos\theta_j\end{pmatrix} \tag{14}$$

Here, ϕ_j, θ_j, and ψ_j are the Euler angles that describe coordinate O_{j-1} in coordinate O_j. The thermal fluctuation of the C–H internuclear vector can therefore be expressed in terms of the time fluctuation of the Euler angles in each frame in the multiple-correlation-time models.

Woessner[11] proposed a motional model corresponding to $p=2$, which is hereafter referred to as 2τ model. In this case the C–H internuclear vector undergoes the diffusional rotation about the z_1 axis in coordinate O_1 and the z_1 axis independently reorients by the isotropic random motion in the laboratory frame. The $J_q(\omega)$ are given by

$$J_q(\omega)=K_q\left[A\frac{2\tau_1}{1+\omega^2\tau_1^2}+B\frac{2\tau_1}{1+\omega^2\tau_1^2}+C\frac{2\tau_2}{1+\omega^2\tau_2^2}\right] \tag{15}$$

with

$$\begin{aligned}\tau_1^{-1}&=\tau_I^{-1}+\tau_R^{-1}\\ \tau_2^{-1}&=\tau_I^{-1}+4\tau_R^{-1}\end{aligned} \tag{16}$$

and

$$\begin{aligned}A&=(3\cos^2\theta_R-1)^2/4\\ B&=3\sin^2\theta_R\cos^2\theta_R\\ C&=(3/4)\sin^2\theta_R\end{aligned} \tag{17}$$

Here, τ_I and τ_R are the correlation times for the isotropic motion and diffusional rotation, respectively, and θ_R is the angle between the C–H internuclear vector and the z_1 axis.

On the other hand, Howarth[12] derived $J_q(\omega)$ for a 3τ model corresponding to $p=3$, where three independent motions are assumed to be superposed for the motion of the C–H internuclear vector as shown in Figure 1. Namely, the C–H vector undergoes the diffusional rotation about the z_1 axis in frame O_1, while the z_1 axis librates within a cone whose axis is parallel to the z_2 axis in frame O_2. Furthermore, the z_2 axis undergoes the isotropic random reorientation in the laboratory frame. Although Howarth[12] employed

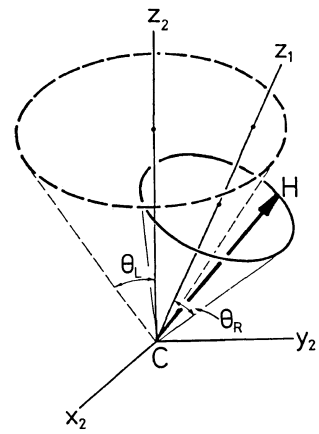

Figure 1. A schematic representation of the 3τ model describing the motion of the C–H internuclear vector.

an empirical approximation, we derived the following equations by the exact mathematical treatment.[9]

$$\begin{aligned}J_q(\omega)=K_q\Big[&A_RA_L\frac{2\tau_I}{1+\omega^2\tau_I^2}+A_R(1-A_L)\\ &\times\frac{2\tau_1}{1+\omega^2\tau_1^2}+B_RB_L\frac{2\tau_2}{1+\omega^2\tau_2^2}\\ &+B_R(1-B_L)\frac{2\tau_3}{1+\omega^2\tau_3^2}+C_RC_L\\ &\times\frac{2\tau_4}{1+\omega^2\tau_4^2}+C_R(1-C_L)\frac{2\tau_5}{1+\omega^2\tau_5^2}\Big]\end{aligned} \tag{18}$$

with

$$\begin{aligned}&\tau_1^{-1}=\tau_I^{-1}+\tau_L^{-1},\ \tau_2^{-1}=\tau_I^{-1}\\ &+\tau_R^{-1},\ \tau_3^{-1}=\tau_I^{-1}+\tau_L^{-1}+\tau_R^{-1},\\ &\tau_4^{-1}=\tau_I^{-1}+4\tau_R^{-1},\ \tau_5^{-1}=\tau_I^{-1}\\ &+\tau_L^{-1}+4\tau_R^{-1},\\ &A_L=\cos^2\theta_L(1+\cos\theta_L)^2/4,\\ &B_L=\sin^2\theta_L(1+\cos\theta_L)^2/6,\\ &C_L=(2+\cos\theta_L)^2(1-\cos\theta_L)^2/24,\\ &A_R=(3\cos^2\theta_R-1)^2/4,\ B_R=3\sin^2\theta_R\cos^2\theta_R,\\ &C_R=3\sin^4\theta_R/4\end{aligned} \tag{19}$$

Here, τ_R, τ_L, and τ_I are the correlation times

for the diffusional rotation, libration, and isotropic random motion, respectively. θ_R and θ_L are the halves of the vertical angles of the cones associated with the corresponding motions. Equation 18 significantly differs from the $J_q(\omega)$ derived by Howarth[12] but both $J_q(\omega)$ are equally reduced to the following equation when $\tau_R \ll \tau_L \ll \tau_I$:[9]

$$J_q(\omega) = K_q\left[A_R A_L \frac{2\tau_I}{1+\omega^2\tau_I^2} + A_R(1-A_L) \times \frac{2\tau_L}{1+\omega^2\tau_L^2} + B_R \frac{2\tau_R}{1+\omega^2\tau_R^2} + C_R \frac{2(\tau_R/4)}{1+\omega^2(\tau_R/4)^2}\right] \quad (20)$$

This equation is expressed as the linear combination of Lorentzian contributions of the respective random motions, if the fourth term is negligible. This indicates that eq 20 becomes a model-free equation for three types of superposed random motions, when the coefficient of each term is assumed to be an adjustable parameter for an analysis. In this paper, however, the exact equation given by eq 18 is employed for the following analysis.

RESULTS

CH_2 Carbons with rrr Tetrads (CH_2(rrr))

The NT_1 and NOE values of CH_2 carbons with *rrr* tetrads are analyzed as the representatives of skeletal carbons because of comparatively large signal intensities. Figure 2 shows the frequency dependence of the NT_1 of CH_2 (*rrr*) carbons for the single-correlation-time model with different τ_cs. Open circles are number-averaged values experimentally obtained at 55°C in $CDCl_3$ solution under different magnetic fields, which were compiled in Table IV in the previous paper.[5] Additional new T_1 data for 125 MHz are also included, which are shown in Table I. Although poor fit

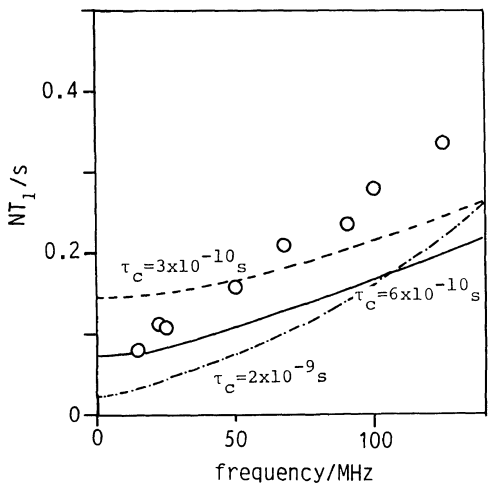

Figure 2. Frequency dependence of NT_1 of the CH_2 (*rrr*) carbon. Open circles are experimental data and the drawn curves indicate the results calculated for the single-correlation-time model.

Table I. ^{13}C T_1 and NOE values of PMMA measured in $CDCl_3$ at 55°C at 125 MHz

Carbon	T_1/s				NOE			
	1	2	3	4	1	2	3	4
α-CH_3 (*rr*)	0.137	0.127	0.144	0.128	2.2	2.01	2.2	2.23
α-CH_3 (*mr*)	0.165	0.157	0.183	0.158	2.3	2.02	2.4	2.49
Quat. C (*rr*)	2.253	2.149	2.40	2.145	1.8	1.51	1.7	1.69
Quat. C (*mr*)	2.441	2.241	2.45	2.317	1.8	1.51	1.3	1.63
OCH_3	1.116	1.071	1.47[a]	0.970	1.7	1.38	1.6	1.60
CH_2 (*rrr*)	0.167	0.146	0.167	0.146	1.8	1.42	1.7	1.63
C=O (*mr*)	1.148	1.093	1.276	1.156	1.3	1.00	1.1	1.04
C=O (*rrrr*)	1.121	0.948	1.129	1.101	1.1	1.00	1.1	1.07
C=O (*mrrr*)	1.154	1.083	1.318	1.102	1.3	1.01	1.1	1.06

[a] Calculated by the non-linear least-squares method. From the linear plot method, a value of 1.64 was obtained.

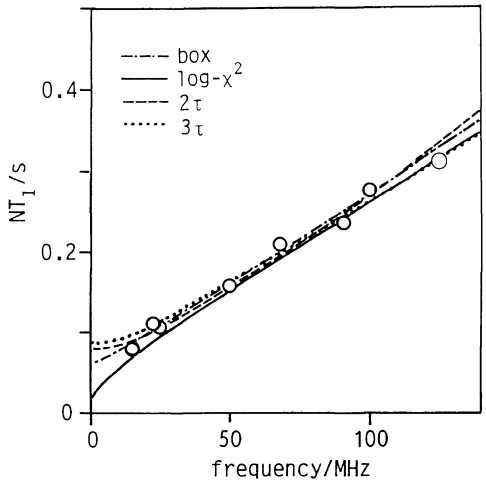

Figure 3. Frequency dependence of NT_1 of the CH_2 (*rrr*) carbon. The curves are the results obtained by the least-squares method using different models for the molecular motion.

Table II. Parameters of different models used for the calculations of NT_1 and NOE values

Carbon	CH_2 (*rrr*)	α-CH_3 (*rr*)	OCH_3
Box-type distribution			
$\bar{\tau}$/s	7.5×10^{-10}	2.1×10^{-10}	—
p	325	144	—
log-χ^2 distribution			
$\bar{\tau}$/s	6.0×10^{-10}	1.0×10^{-10}	—
p	10.0	20.0	—
b	100	100	
2τ model			
τ_R/s	2.0×10^{-12}	2.0×10^{-12}	2.0×10^{-12}
θ_R/degree	24.6	26.5	65.9
τ_I/s	1.0×10^{-9}	4.0×10^{-10}	4.4×10^{-10}
3τ model			
τ_R/s	2.0×10^{-12}	2.0×10^{-12}	1.0×10^{-12}
θ_R/degree	15.7	17.7	64.7
τ_L/s	1.1×10^{-10}	1.2×10^{-10}	1.0×10^{-11}
θ_L/degree	31.2	47.9	9.9
τ_I/s	1.0×10^{-9}	7.7×10^{-10}	8.0×10^{-10}

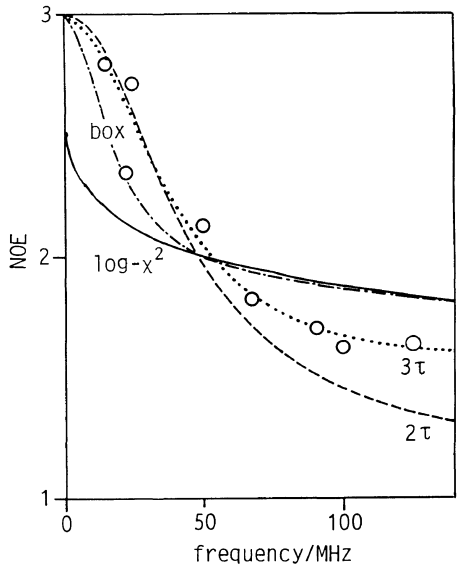

Figure 4. Frequency dependence of NOE of the CH_2 (*rrr*) carbon. The curves are the results calculated using the same parameters for the respective models as for the T_1 data shown in Figure 3.

is obtained for any τ_c, the slope of the frequency dependence for $\tau_c = 2\times10^{-9}$ s seems to be very close to that of the experimental results.

Figures 3 and 4 show the frequency dependencies of NT_1 and NOE values estimated using 2τ and 3τ models as well as box-type and log-χ^2 type distribution models. The respective curves were determined by mainly trying to obtain best fits for NT_1 data by the nonlinear least-squares method on a computer. The NT_1 results calculated for every model are in good accord with the experimental data, though some minor deviation appears in both lower and higher frequencies depending on the molecular motional models. In contrast, the NOE values calculated using the same parameters as for NT_1 greatly differ from model to model, and only the 3 model is found to give the best fit with the experimental values among these models.

On the other hand, similar good fits were also obtained for the frequency dependence of NOE in the respective models except for the single-correlation-time model, when the non-linear least-squares method was exclusively applied to the NOE values. In this case, however, only the 3τ model could reproduce well the T_1 values using the same parameters as for NOE. It is, therefore, concluded that the 3τ model is the most plausible model describing

the frequency dependences of NT_1 and NOE for the CH_2 carbons with *rrr* tetrads.

In Table II are summarized parameters of different models used for the calculations of NT_1 and NOE values. The parameters for the 3τ model were determined to obtain the best fits with both T_1 and NOE values, while those for the other models were obtained so as to reproduce the T_1 values.

α-CH_3 Carbons with rr Triads: α-CH_3 (rr)

α-CH_3 carbons with *rr* triads are analyzed as the representatives of the side-chain carbons directly bonded to skeletal carbons. Figures 5 and 6 show the results of NT_1 and NOE of α-CH_3 (*rr*) carbons. Here, the experimental data are somewhat dispersed compared to the cases of the CH_2 (*rrr*) carbons. Although such dispersion may induce the minor difference in fitness for the respective motional models, the T_1 values calculated for those models fairly well agree with the experimental values. On the other hand, in the case of NOE the difference among the models is prominent, and the data calculated for the 3τ model seem to also give the best fit with the experimental data.

OCH_3

Finally, OCH_3 carbons are analyzed; they are the side-chain carbons far from sketetal carbons. In Figures 7 and 8 are shown the results of NT_1 and NOE for OCH_3 carbons. As is clearly seen in Figure 7, the T_1 values are more than 1s in this frequency range. Such high T_1 values were not interpreted in terms of any model considering a wide distribution of the

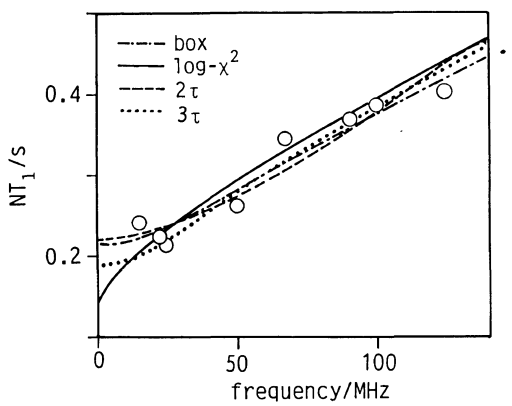

Figure 5. Frequency dependence of NT_1 of the α-CH_3 (*rr*) carbon. The curves are the results obtained by the least-squares method using different models for the molecular motion.

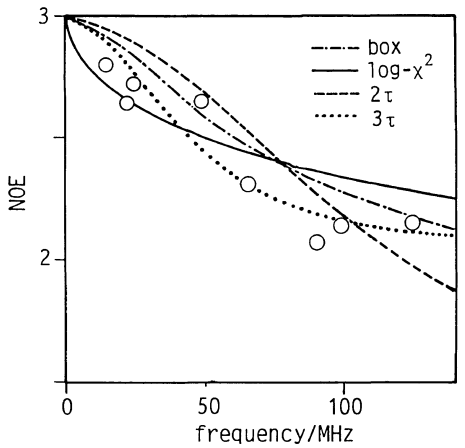

Figure 6. Frequency dependence of NOE of the α-CH_3 (*rr*) carbon. The curves are the results calculated using the same parameters for the respective models as for the T_1 data shown in Figure 5.

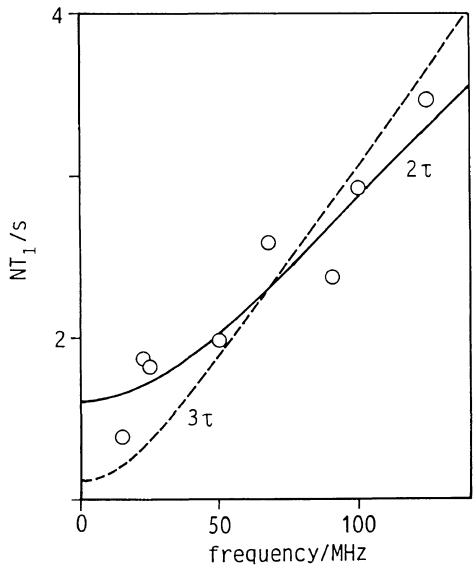

Figure 7. Frequency dependence of NT_1 of the OCH_3 carbon. The curves are the results obtained by the least-squares method using 2τ and 3τ models.

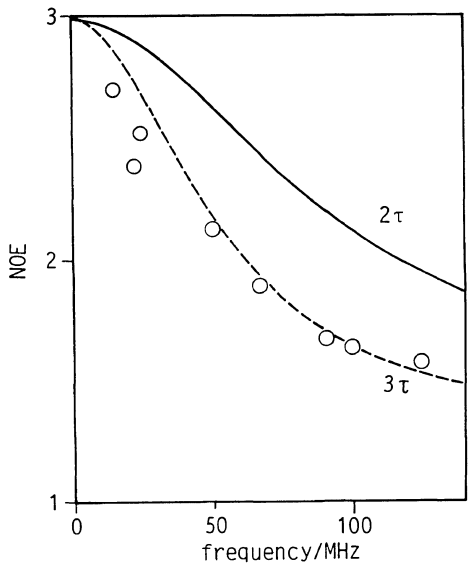

Figure 8. Frequency dependence of NOE of the OCH_3 carbon. The curves are the results calculated using the same parameters for 2τ and 3τ models as for the T_1 data shown in Figure 7.

correlation time. 2τ and 3τ models seem to be appropriate for describing the frequency dependence of T_1 values, although the reproduced curves are significantly different for these two models due to the dispersion of the experimental data. In contrast, the frequency dependence of NOE is found to be interpreted in terms of the 3τ model, whereas the 2τ model cannot reproduce the experimental data of NOE.

DISCUSSION

According to our preliminary measurements, ^{13}C T_1s of the respective carbons for the same PMMA solution as used in this work increase with increasing temperature at the temperature range from room temperature to 55°C at a frequency of 100 MHz. This indicates that the system treated in this work should be on the higher temperature side with respect to the T_1 minima which may appear in observing a temperature dependence of T_1 at frequencies at least less than 100 MHz. Nevertheless, we have found such significant frequency dependences of T_1 values as shown in Figures 2, 5, and 7. This strongly suggests that the single correlation time theory is inadequate, because the frequency dependence will disappear under the so-called extreme narrowing condition, which corresponds to the higher temperature side of the T_1 minimum, in this theory.

As already described in the case of CH_2 (*rrr*) carbons, the frequency dependences of T_1 and NOE can be interpreted in terms of the box-type or log-χ^2 distribution model when they are independently tried to fit experimental data by the least-squares method. However, it is impossible to obtain the best fits for both frequency dependences using the same parameters describing the average correlation times and their distributions in these models. The situation is the same for the 2τ model; there is no parameter to sufficiently reproduce both T_1 and NOE values. These imply that monomodal wide distributions of correlation times and two discrete correlation times are not adequate to describe the complicated molecular motions of PMMA chains in solution.

In contrast, Heatley and Begum[1] reported that the temperature dependeces of T_1 and NOE could be explained for the respective protonated carbons of PMMA in solution in terms of either the Cole–Cole distribution of correlation times, the log-χ^2 distribution or a conformational jump model of chain dynamics. Here, the conformational jump model, in which the C–H internuclear vector undergoes a combined motion of conformational jumps and overall molecular tumbling, may correspond to our 2τ model. In their case they analyzed the temperature dependencies of relaxation data at a fixed frequency of 25.14 MHz. Such an analysis may be less reliable compared to our analysis of the frequency dependences even if the temperature is fixed in our case.

The 3τ model has been found to be the most adequate to interpret the frequency dependences of T_1 and NOE values for the protonated carbons of PMMA in this work.

Similar 3τ model analyses were successfully performed for the temperature dependences of T_1, NOE and spin–spin relaxation time (T_2) values of CH_2 carbons of the noncrystalline components which are contained in bulk-crystallized and solution-grown polyethylene samples.[13] Moreover, molecular motions of methylene sequences of a series of terephthalic-acid polyesters $(COC_6H_4COO(CH_2)_mO)_n$ with different number m of methylene carbons were also examined at temperatures above the glass transition temperatures by the 3τ model analysis.[14,15] On the basis of these results, the respective motions assumed in the 3τ model may be assigned as follows. The diffusional rotation should be the torsional motion about C–C bonds with no activation energy, which may be the cooperative motion associating with several methylene sequences. The librational motion should be ascribed to a restricted motion involving some transitions between *trans* and *gauche* conformations which will be allowable for a relatively short methylene sequence. On the other hand, the isotropic motion may be still a restricted motion but longer methylene sequences are thought to be associated with this motion with a higher activation energy compared to the case of the librational motion.

The same assignment may be applicable to the respective motions of the backbone CH_2 (*rrr*) carbons of PMMA in solution, although the angles θ_R and θ_L for the diffusional rotation and the libration, which will describe the amplitudes for the respective motions, should somewhat differ from the values ($\theta_R = 33°$ and $\theta_L = 63°$)[13] for the methylene sequences in the rubbery state. The differences in θ_R and θ_L suggest the differences in flexibilities of the sequences which are associated with the corresponding local motions. However, these values are adjustable parameters for the least-squares analysis and cannot be used for discussing the detailed structure for polymeric chains.

The frequency dependences of T_1 and NOE values of side group α-CH_3 (*rr*) and OCH_3 carbons have also been well interpreted in terms of the 3τ model. Nevertheless, such good agreements with experimental and calculated data should be superficial for these carbons, because additional independent motions may be allowable for the side groups compared to the case of backbone carbons. In α-CH_3 (*rr*) carbons, the θ_L value significantly differs from the value of the CH_2 (*rrr*) carbon as shown in Table II. This would indicate that the rotation of α-CH_3 groups with the correlation time of 10^{-10} s happen to overlap the librational motion of the backbone carbons. Such a rate of the α-CH_3 rotation is significantly higher than that in the glassy state which was revealed for PMMA using a similar ^{13}C T_1 analysis.[10] On the other hand, θ_R and θ_L as well as τ_L for OCH_3 carbons are much different from those values of the backbone carbons as is seen in Table II. This suggests that OCH_3 carbons may additionally undergo the methyl rotation and another rotation whose correlation times are of the orders of 10^{-12} and 10^{-11} s. More detailed characterization of side-group motions will be carried out using a 4τ or 5τ model. In such cases temperature dependencies of T_1 and NOE values should be measured under several static magnetic fields to increase the reliability of the analyses.

REFERENCES

1. F. Heatley and A. Begum, *Polymer*, **17**, 399 (1976).
2. (a) P. Dais, M. E. Nedea, F. G. Morin, and R. H. Marchessault, *Macromolecules*, **22**, 4208 (1989). (b) P. Dais, M. E. Nedea, F. G. Morin, and R. H. Marchessault, *Macromolecules*, **23**, 3387 (1990).
3. (a) S. Glowinkowski, D. J. Gisser, and M. D. Ediger, *Macromolecules*, **23**, 3520 (1990). (b) D. J. Gisser, S. Glowinkowski, and M. D. Ediger, *Macromolecules*, **24**, 4270 (1991); recent related papers therein.
4. R. Chûjô, K. Hatada, R. Kitamaru, T. Kitayama, H. Sato, Y. Tanaka, F. Horii, and Y. Terawaki, *Polym. J.*, **20**, 627 (1988).
5. R. Chûjô, K. Hatada, R. Kitamaru, T. Kitayama, H. Sato, and Y. Tanaka, *Polym. J.*, **19**, 413 (1987).
6. R. Chûjô, *Makromol. Chem., Makromol. Symp.*, **34**, 59 (1990).

7. A. W. Nolle and J. J. Billings, *J. Chem. Phys.*, **30**, 84 (1959).
8. J. Schaefer, *Macromolecules*, **6**, 882 (1973).
9. K. Murayama, F. Horii, and R. Kitamaru, *Bull. Inst. Chem. Res., Kyoto Univ.*, **61**, 229 (1983).
10. F. Horii, Y. Chen, M. Nakagawa, B. Gabrys, and R. Kitamaru, *Bull. Inst. Chem. Res., Kyoto Univ.*, **66**, 317 (1988).
11. D. E. Woessner, *J. Chem. Phys.*, **36**, 1 (1962).
12. O. W. Howarth, *J. Chem. Soc., Faraday Trans. 2*, **75**, 863 (1979).
13. F. Horii, K. Murayama, and R. Kitamaru, *Polym. Prepr. Jpn.*, **31**, 2509 (1982).
14. F. Horii, A. Hirai, K. Murayama, R. Kitamaru, and T. Suzuki, *Macromoleules*, **16**, 273 (1983).
15. T. Murata, F. Horii, and H. Odani, *Polym. Prepr. Jpn.*, **39**, 1055 (1990).